Rare-Earth-Mediated Optomechanical System in the Reversed Dissipation Regime

Ryuichi Ohta,[1] Loïc Herpin,[1] Victor M. Bastidas,[1,2] Takehiko Tawara,[1,3]
Hiroshi Yamaguchi,[1] and Hajime Okamoto[1]

[1]*NTT Basic Research Laboratories, NTT Corporation, 3-1 Morinosato Wakamiya, Atsugi-shi, Kanagawa 243-0198, Japan*
[2]*NTT Research Center for Theoretical Quantum Physics, NTT Corporation, 3-1 Morinosato Wakamiya, Atsugi-shi, Kanagawa 243-0198, Japan*
[3]*NTT Nanophotonics Center, NTT Corporation, 3-1 Morinosato Wakamiya, Atsugi-shi, Kanagawa 243-0198, Japan*

(Received 24 June 2020; revised 16 September 2020; accepted 5 January 2021; published 29 January 2021)

Strain-mediated interaction between phonons and telecom photons is demonstrated using excited states of erbium ions embedded in a mechanical resonator. Owing to the extremely long-lived nature of rare-earth ions, the dissipation rate of the optical resonance falls below that of the mechanical one. Thus, a "reversed dissipation regime" is achieved in the optical frequency region. We experimentally demonstrate an optomechanical coupling rate $g_0 = 2\pi \times 21.7$ Hz, and numerically reveal that the interaction causes stimulated excitation of erbium ions. Numerical analyses further indicate the possibility of g_0 exceeding the dissipation rates of erbium and mechanical systems, thereby leading to single-photon strong coupling. This strain-mediated interaction, moreover, involves the spin degree of freedom, and has a potential to be extended to highly coherent opto-electro-mechanical hybrid systems in the reversed dissipation regime.

DOI: 10.1103/PhysRevLett.126.047404

Interactions between electromagnetic and acoustic waves have been investigated through various optical resonances, such as optical cavities [1–4], microwave circuits [5–8], and solid-state two-level systems [9–16], incorporated in mechanical resonators. Recently, these optomechanical interactions have attracted much attention in diverse fields ranging from quantum information to nonlinear optics. Sideband cooling of the mechanical mode to its ground state [1], coherent energy transfer between photons and phonons [2,3,6], and generation of their entangled states [4] have been demonstrated in the past decade.

In these systems, the dissipation rates of the optical and mechanical resonances are of crucial importance to determining the dynamics of the photons and phonons. For instance, to optically cool (readout) the mechanical motion (phonon state), the dissipation rate of the optical resonance should be larger than that of the mechanical one ($\gamma_{\mathrm{opt}} > \gamma_m$). This regime is the conventional situation in cavity optomechanical systems. In contrast, the opposite situation ($\gamma_{\mathrm{opt}} < \gamma_m$) inverts the roles of photons and phonons. In this regime, the optical resonance and its intraphoton are dominantly affected by the dynamic backaction of the optomechanical interaction, which leads to quantum-limited amplification and self-oscillation of photons [8,17], entangled-photon generation [18], and reservoir engineering of photons for nonreciprocal manipulations [19,20]. So far, this reversed dissipation regime has been realized in the microwave region [8]. However, it is difficult to achieve in the optical region, including telecom wavelengths which enable long-distance communication. The main obstacle is the large energy difference between photons and phonons. Although high-Q optical cavities have been incorporated in optomechanical systems, their dissipation rates are of the order of a megahertz, i.e., much higher than mechanical dissipation rates, which typically range from a hertz to a kilohertz. The optomechanical interaction using the long-lived optical resonance, whose dissipation rate is lower than that of the mechanical one, is required to achieve the reversed dissipation regime in the optical region.

In this Letter, we demonstrate strain-mediated optomechanical interaction between erbium (Er) ions and a Y_2SiO_5 (YSO) mechanical resonator. The excited states of the Er ions play the role of the optical resonance whose dissipation rate γ_{Er} falls below $2\pi \times 99$ Hz (corresponding $Q > 10^{13}$). Their very low dissipation rate is owing to the $4f$-$4f$ transition of the rare-earth ions, which is originally forbidden by the dipole selection rule. This dissipation rate is 5 orders of magnitude lower than those of the optical resonances in the conventional optomechanical systems, such as cavities [1–4] and other two-level systems [10–16], and one order of magnitude lower than that of the mechanical resonator in this study. Therefore, we achieved the reversed dissipation regime at telecom wavelength, where the mechanical energy relaxation rate exceeds the energy decay rate of the Er ions ($\gamma_{\mathrm{Er}} < \gamma_m$).

In contrast to the reported two-level systems [9–16], the optical resonance of Er ions is considered to be less influenced by the environmental perturbations because it originates from the inner shell orbits. One important aspect of our work is that we experimentally observed the energy modulations driven by the mechanical

deformation. These results revealed the dispersive interaction between Er ions and mechanical motion, where the coupling rate $g_0 = 2\pi \times 21.7$ Hz was determined from the experiments. We theoretically investigated this optomechanical system by using the master equation approach and found that the strain-mediated interaction caused stimulated excitation of Er ions with a blue-detuned pump. Further numerical simulations indicated that g_0 could be enhanced to exceed the dissipation rates of the optical and mechanical resonances, leading to strong coupling between a single photon and phonon ($\gamma_{\mathrm{Er}} < \gamma_m < g_0$). The strain-mediated interaction moreover presents the possibility of manipulating the Er ions without external microwaves, which is advantageous to on-chip integration of quantum systems for information and sensing applications [21]. These results pave the way to nonlinear manipulation and reservoir engineering of photons, as well as highly coherent hybrid systems in the reversed dissipation regime.

The Er ions in this study were uniformly doped in bulk YSO crystals (provided by Scientific Materials). The concentration of Er ions was 0.1%. The degeneracy of each energy level is lifted because of the crystal fields of YSO. Mechanical deformation of YSO geometrically perturbs its crystal field and the transition energies between $I_{15/2}$ and $I_{13/2}$ levels, which is the origin of the strain-mediated optomechanical interaction in this scheme [Fig. 1(a)]. Static strain effects of Er:YSO have been studied with codoping of other rare-earth materials, such as Eu [22] and Sc [23]. These auxiliary impurities randomly generate local strain and increase the inhomogeneous linewidths of the Er ions. Previous experiments have demonstrated that the applied strain does not degrade the coherence of the excited states of the Er ions [22]. Therefore, small dephasing rates ($\gamma_2 < 1$ kHz [22,24]) can be obtained under strain.

We fabricated mechanical resonators by using angled focused ion beam milling [25,26]. Figure 1(b) is a scanning electron microscope (SEM) image of a fabricated resonator taken from the top. Length, width, and milling angle were 160 μm, 16 μm, and 45°, respectively. The length, width, and height were directed to the D_1, D_2, and b axes of the crystal. The sample was mounted on a piezoactuator, which electrically drove the mechanical motion, and it was cooled to a temperature of 4 K.

The mechanical properties of the fabricated resonators were obtained with a HeNe laser and a Doppler interferometer, which allows us to measure the velocity and obtain the displacement of the motion. In the following measurements, we electrically drove the second-order flexural mode of the resonator [11], whose maximum strain is located at the midpoint. Figure 1(c) shows the frequency response of this mode measured at the midpoint of the resonator. The mechanical resonance frequency and quality factor were 1.57 MHz and 2500.

The optical properties of the excited states of the Er ions were investigated through photoluminescence excitation (PLE) measurements. We excited the Y_1-Z_1 transition (1536.4 nm) of the doped Er ions at site 1 of the crystal

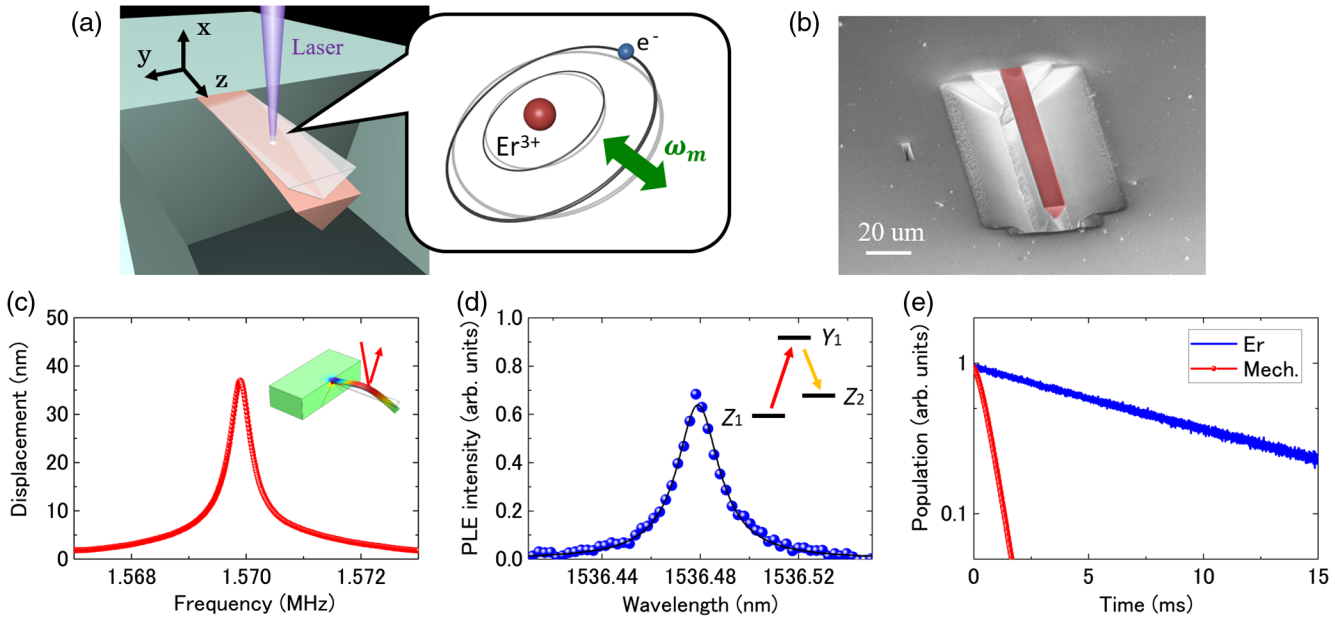

FIG. 1. (a) Schematic image of the strain-mediated optomechanical interaction of Er ions in a mechanical resonator. The mechanical vibration modulates the transition energy of the Er ions. (b) SEM image of Er:YSO mechanical resonator (red shaded region). (c) Measured frequency response of the second-order flexual mode of the resonator. The inset shows the shape and strain distribution of this mode calculated by FEM. (d) PLE spectrum of the Y_1-Z_1 transition of the Er ions embedded in the resonator. The inset shows the energy diagram of this transition. (e) Energy decay of the excited state of Er ions and the mechanical mode. The dissipation rate of the Er ions is one order of magnitude lower than that of the mechanical mode.

and measured the luminescence from their Y_1-Z_2 transition (1546.5 nm). The laser was aligned along the b axis and was focused on the midpoint and the top surface of the resonator. The focal depth of the objective lens was about 3 μm, so that about 1×10^9-Er ions were located in the laser spot. Figure 1(d) depicts the PLE spectrum of the Er ions embedded in the resonator without mechanical drive. The linewidth was 2.66 GHz, which indicated intrinsic inhomogeneous broadening of the transition energies.

The dissipation rates of the Er ions and the mechanical resonance were independently evaluated by the ring-down measurements using the same Er:YSO resonator with the same conditions, where the pump pulse width and period were longer than the dissipation rates. Figure 1(e) shows the energy decays of the excited state of the Er ions and the second-order flexural mode of the resonator. The decay times of the Er ions and the mechanical mode were 10.1 and 0.56 ms, respectively, where the corresponding dissipation rates were $\gamma_{\mathrm{Er}} = 2\pi \times 99$ Hz and $\gamma_m = 2\pi \times 1.79$ kHz. The dissipation rate of Er ions was one order of magnitude lower than that of the mechanical mode, which satisfies the criteria of the reversed dissipation regime ($\gamma_{\mathrm{Er}} < \gamma_m$).

We experimentally demonstrated the strain-mediated optomechanical interaction in this reversed dissipation regime by making PLE measurements under mechanical vibration. First, we continuously measured the PLE spectra at a drive voltage of 20 V_{pp}, which generated a peak-to-peak mechanical displacement $x_{pp} = 357$ nm at the resonance frequency. The drive frequency dependences shown in Fig. 2 reveal that the vibrational strain significantly

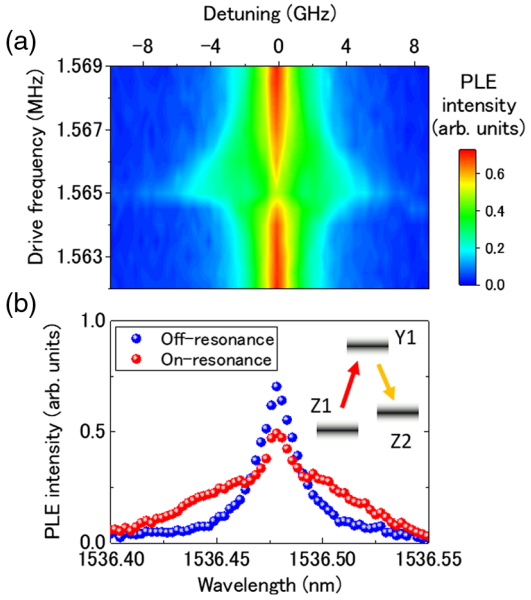

FIG. 2. (a) Drive frequency dependence of PLE spectra taken with continuous excitation of the pump laser. (b) PLE spectra at on- (red) and off-resonance (blue). The inset is a schematic image of the energy diagram with mechanical vibration.

broadened the PLE spectra. This peak broadening was due to the time averaging of the continuously modulated transition energy of Er ions and increase in the inhomogeneous linewidth [27]. The full-width at half-maximum (FWHM) of this broadening was 10.5 GHz.

To evaluate the optomechanical coupling factors, we performed stroboscopic PLE measurements. In this scheme, the intensity of the excitation laser was modulated to define the pulse shape, whose repetition was synchronized to the mechanical resonance frequency [Fig. 3(a)]. Therefore, by changing the relative phase of the pump pulse and mechanical motion, we could measure the PLE spectra at arbitrary times of the mechanical motion. Figures 3(b)–3(d) show the stroboscopic PLE spectra at different drive voltages, $V_d = 3$, 5, and 10 V_{pp}, where the measured x_{pp} were, respectively, 103, 193, and 289 nm. The mechanical strain clearly modulated the transition energies of the Er ions. The sinusoidally modulated spectra, instead of the periodic peak broadening, indicate that the excitation laser was well focused on the top surface of the resonator [27]. We evaluated the dispersive optomechanical coupling factors from the peak fittings with Eq. (1) in Figs. 3(b)–3(d).

$$\omega_{\mathrm{Er}} = \omega_0 + \frac{G_{\mathrm{disp}} x_{pp}}{2} \sin(\omega_m t + \theta_0) \ . \tag{1}$$

Here, ω_0 is the steady-state transition energy of the Er ions, G_{disp} is the coupling factor normalized by the mechanical displacement, ω_m represents the resonance frequency of the mechanical mode, and θ_0 is the phase difference between the pump laser and the mechanical motion. Figure 3(e) shows the displacement and corresponding stress dependences of the frequency shifts, where the corresponding stress was numerically calculated with the finite element method (FEM). The linear dependence of the energy shift gives $G_{\mathrm{disp}} = 27$ MHz/nm. To compare the magnitude of the optomechanical interaction of Er ions to those of other two-level systems, we also derived the structural independent coupling factor G_{stress}, which corresponds to the energy shift normalized by stress. For Er ions, G_{stress} is 243 Hz/Pa, which is as large as those of NV centers (465 Hz/Pa [31]), while the dissipation rate of the excited states of Er ions is 6 orders of magnitude smaller than that of NV centers. The optomechanical coupling rate g_0 in this system is derived from the energy shift caused by a single-phonon fluctuation.

$$g_0 = G_{\mathrm{disp}} x_{\mathrm{ZPF}}, \tag{2a}$$

$$x_{\mathrm{ZPF}} = \sqrt{\frac{\hbar}{2 m_{\mathrm{eff}} \omega_m}}. \tag{2b}$$

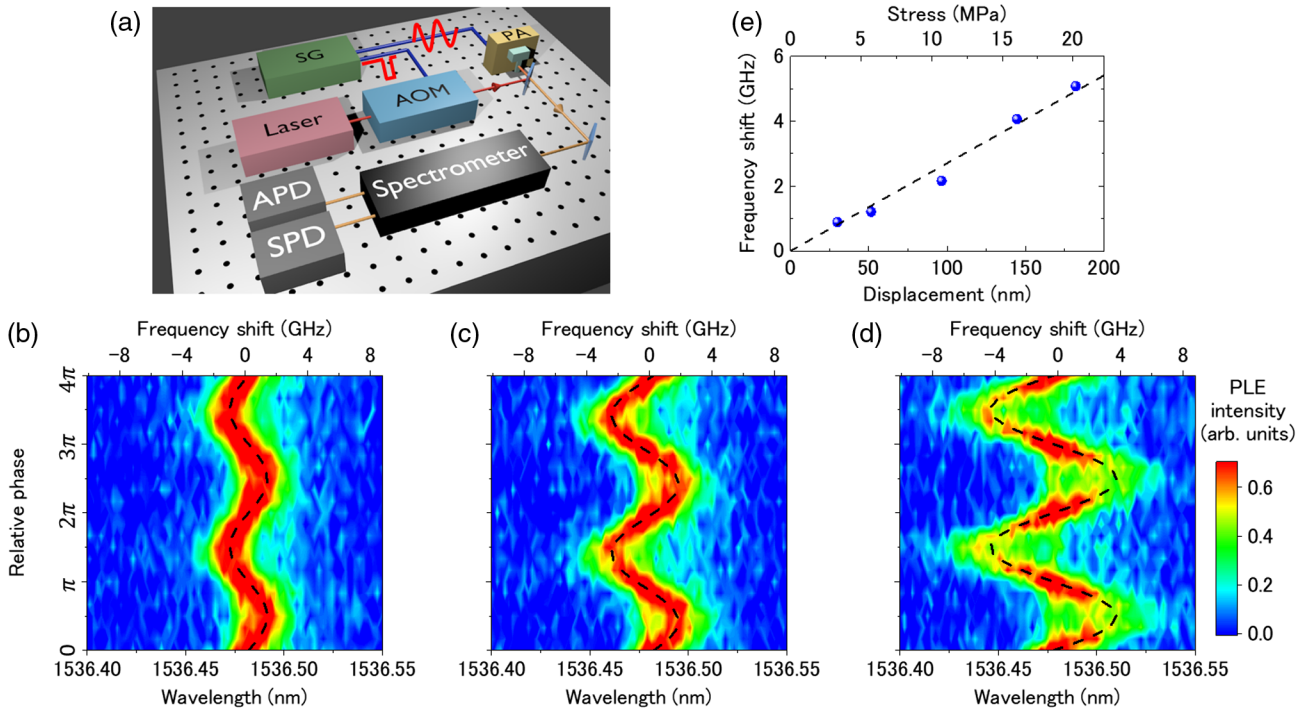

FIG. 3. (a) Schematic image of stroboscopic measurement. AOM: acousto-optical modulator; SG: signal generator; PA: piezoactuator; APD: avalanche photodiode; SPD: single-photon detector. (b)–(d) stroboscopic PLE spectra at drive voltages of 3 (b), 5 (c), and 10 V_{pp} (d), where the measured displacements (x_{pp}) were 103, 193, 289 nm, respectively. The vertical axes correspond to the relative phase of the pump laser and mechanical motion. Dashed lines are curves fitted with Eq. (1). (e) Mechanical displacement and stress dependences of the frequency shifts of the transition energy of Er ions fitted by a linear function (dashed line).

Here, the zero-point fluctuation x_{ZPF} and effective mass of the resonator m_{eff} are 0.78 fm and 8.6 ng, respectively. Thus, we experimentally obtained $g_0 = 2\pi \times 21.7$ Hz for our optomechanical system.

As discussed in Refs. [8] and [17], the dispersive optomechanical (OM) interaction in the reversed dissipation regime modifies the susceptibility of the optical resonance and leads to amplification and lasing of the cavity photons with a blue-detuned pump. Here, we theoretically discuss the backaction effects of the dispersive interaction between an ensemble Er ions and a mechanical resonator by using the master equation [27,32,33]. In this model, we assume that the mechanical motion collectively interacts with the ensemble Er ions, that the occupancy of their excited states is much lower than unity, and that the inhomogeneity of ω_{Er} becomes small enough to use a blue-detuned pump [27].

$$\hat{H}_{\mathrm{OM}} = -\Delta_0 \hat{a}^\dagger \hat{a} + \omega_m \hat{b}^\dagger \hat{b} - g_0 \hat{a}^\dagger \hat{a}(\hat{b}^\dagger + \hat{b}) + \Omega\sqrt{N}(\hat{a}^\dagger + \hat{a}), \tag{3a}$$

$$\dot{\hat{\rho}} = i[\hat{H}_{\mathrm{OM}}, \hat{\rho}] + \frac{\gamma_1}{2}\mathcal{D}(\hat{a})\hat{\rho} + \frac{\gamma_2}{2}\mathcal{D}(\hat{a}^\dagger \hat{a})\hat{\rho} + \frac{\gamma_m}{2}\mathcal{D}(\hat{b})\hat{\rho}. \tag{3b}$$

Here, $\hat{a}$ ($\hat{a}^\dagger$) and $\hat{b}$ ($\hat{b}^\dagger$) are the annihilation (creation) operators of Er ions and phonons, $\Delta_0 = \omega_L - \omega_{\mathrm{Er}}$ is the detuning between the pump and transition frequency, N is the number of the Er ions in the laser spot, Ω is the pump amplitude, $\hat{\rho}$ is the density matrix, $\gamma_1 = 2\pi \times 99$ Hz and $\gamma_2 = 2\pi \times 1$ kHz [22,24] are the dissipation and dephasing rates of Er ions, and $\mathcal{D}(\hat{O})\hat{\rho} = 2\hat{O}\hat{\rho}\hat{O}^\dagger - \hat{O}^\dagger\hat{O}\hat{\rho} - \hat{\rho}\hat{O}^\dagger\hat{O}$ for a given operator $\hat{O}$. Figure 4 shows that the effective damping rate of the Er ions (γ_{eff}) decreases as a function of the number of excited ions ($n_{\mathrm{Er}} = |\bar{a}|^2$) generated by the blue-detuned pump. This optomechanical interaction simultaneously amplifies the excitation efficiency of Er

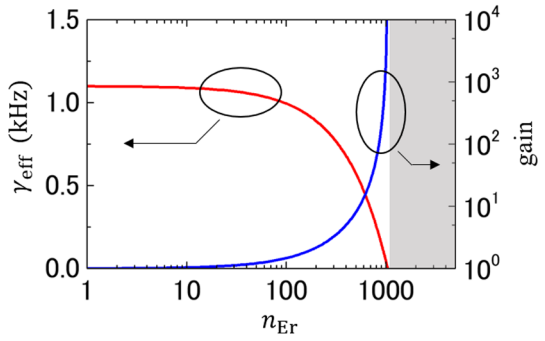

FIG. 4. Gain and effective damping rate as a function of n_{Er} with blue-detuned pump. Shaded area indicates the region of the self-sustained oscillation.

ions (gain), which leads to self-sustained oscillation of Er ions in analogy with the optomechanically induced instabilities [8,17].

The interaction between the low-loss optical and mechanical resonances has prospects for quantum and many-body physics. As described in Eq. (2), g_0 in this system increases as the effective mass of the resonator decreases. We numerically derived that g_0 reaches $2\pi \times 2$ kHz and exceeds both dissipation rates for a resonator whose length and width are 20 μm and 1 μm [27], which are still large enough to be fabricated with this method. In this regime, a single photon can be strongly coupled to a single phonon, whereas the reported optomechanical strong couplings have been achieved with multiple photons to amplify the effective coupling rate [5,34,35]. Such a small resonator may cause experimental difficulties in terms of optical readout of the Er ions, because the number of Er ions decreases as the volume decreases. However, the difficulties would be solved by integrating optical components, such as waveguides and couplers [24,25,36], which drastically improve the overall transduction to the Er ions. This single-photon strong coupling enables one to construct multipartite entangled spin systems in a solid-state platform [37].

In conclusion, we experimentally demonstrated a strain-mediated interaction between the optical resonance of Er ions and a mechanical resonator. The long-lived excited states of Er ions enabled us to reach the reversed dissipation regime at telecom wavelengths, which applies backaction on the optical resonance and amplifies the excitation rate of the Er ions. The extremely small dissipation of Er ions has a potential to provide strong coupling between a single photon and phonon. Our results offer new directions for research into optomechanical physics and will pave the way to coherent manipulation of photons, phonons, and even electrons in the reversed dissipation regime.

We thank M. Hiraishi, T. Inaba, X. Xu, M. Asano, H. Toida, M. Ono, S. Kita, W. J. Munro, and K. Nemoto for technical support and fruitful discussions.

[1] J. Chan, T. P. M. Alegre, A. H. Safavi-Naeini, J. T. Hill, A. Krause, S. Gröblacher, M. Aspelmeyer, and O. Painter, Nature (London) **478**, 89 (2011).

[2] R. W. Andrews, R. W. Peterson, T. P. Purdy, K. Cicak, R. W. Simmonds, C. A. Regal, and K. W. Lehnert, Nat. Phys. **10**, 321 (2014).

[3] M. Forsch, R. Stockill, A. Wallucks, I. Marinkovic, C. Gärtner, R. A. Norte, F. van Otten, A. Fiore, K. Srinivasan, and S. Gröblacher, Nat. Phys. **16**, 69 (2020).

[4] R. Riedinger, A. Wallucks, I. Marinkovic, C. Löschnauer, M. Aspelmeyer, S. Hong, and S. Gröblacher, Nature (London) **556**, 473 (2018).

[5] J. D. Teufel, D. Li, M. S. Allman, K. Cicak, A. J. Sirois, J. D. Whittaker, and R. W. Simmonds, Nature (London) **471**, 204 (2011).

[6] T. Bagci, A. Simonsen, S. Schmid, L. G. Villanueva, E. Zeuthen, J. Appel, J. M. Taylor, A. Sørensen, K. Usami, A. Schliesser, and E. S. Polzik, Nature (London) **507**, 81 (2014).

[7] C. F. Ockeloen-Korppi, E. Damskägg, J.-M. Pirkkalainen, M. Asjad, A. A. Clerk, F. Massel, M. J. Woolley, and M. A. Sillanpää, Nature (London) **556**, 478 (2018).

[8] L. D. Toth, N. R. Bernier, A. Nunnenkamp, A. K. Feofanov, and T. J. Kippenberg, Nat. Phys. **13**, 787 (2017).

[9] Y. Chu, P. Kharel, W. H. Renninger, L. D. Burkhart, L. Frunzio, P. T. Rakich, and R. J. Schoelkopf, Science **358**, 199 (2017).

[10] I. Yeo, P.-L. de Assis, A. Gloppe, E. Dupont-Ferrier, P. Verlot, N. S. Malik, E. Dupuy, J. Claudon, J-M. Gérard, A. Auffèves, G. Nogues, S. Seidelin, J-Ph. Poizat, O. Arcizet, and M. Richard, Nat. Nanotechnol. **9**, 106 (2014).

[11] M. Montinaro, G. Wüst, M. Munsch, Y. Fontana, E. Russo-Averchi, M. Heiss, A. F. i Morral, R. J. Warburton, and M. Poggio, Nano Lett. **14**, 4454 (2014).

[12] M. Weiß, J. B. Kinzel, F. J. R. Schülein, M. Heigl, D. Rudolph, S. Morkötter, M. Döblinger, M. Bichler, G. Abstreiter, J. J. Finley, G. Kolmüller, A. Wixforth, and H. J. Krenner, Nano Lett. **14**, 2256 (2014).

[13] M. Metcalfe, S. M. Carr, A. Muller, G. S. Solomon, and J. Lawall, Phys. Rev. Lett. **105**, 037401 (2010).

[14] A. Barfuss, J. Teissier, E. Neu, A. Nunnenkamp, and P. Maletinsky, Nat. Phys. **11**, 820 (2015).

[15] H. Y. Chen, E. R. MacQuarrie, and G. D. Fuchs, Phys. Rev. Lett. **120**, 167401 (2018).

[16] R. Ohta, H. Okamoto, T. Tawara, H. Gotoh, and H. Yamaguchi, Phys. Rev. Lett. **120**, 267401 (2018).

[17] A. Nunnenkamp, V. Sudhir, A. K. Feofanov, A. Roulet, and T. J. Kippenberg, Phys. Rev. Lett. **113**, 023604 (2014).

[18] Y. D. Wang and A. A. Clerk, Phys. Rev. Lett. **110**, 253601 (2013).

[19] A. Metelmann and A. A. Clerk, Phys. Rev. X **5**, 021025 (2015).

[20] K. Fang, A. Metelmann, M. H. Matheny, F. Marquardt, A. A. Clerk, and O. Painter, Nat. Phys. **13**, 465 (2017).

[21] D. D. Awschalom, R. Hanson, J. Wrachtrup, and B. B. Zhou, Nat. Photonics **12**, 516 (2018).

[22] T. Böttger, C. W. Thiel, R. L. Cone, and Y. Sun, Phys. Rev. B **77**, 155125 (2008).

[23] S. Welinski, C. W. Thiel, J. Dajczgewand, A. Ferrier, R. L. Cone, R. M. Macfarlane, T. Chanelière, A. Louchet-Chauvet, and P. Goldner, Opt. Mater. **63**, 69 (2017).

[24] T. Böttger, C. W. Thiel, Y. Sun, and R. L. Cone, Phys. Rev. B **73**, 075101 (2006).

[25] T. Zhong, J. Rochman, J. M. Kindem, E. Miyazono, and A. Faraon, Opt. Express **24**, 536 (2016).

[26] T. Zhong, J. M. Kindem, J. G. Bartholomew, J. Rochman, I. Craiciu, E. Miyazono, M. Bettinelli, E. Cavalli, V. Verma, S. W. Nam, F. Marsili, M. D. Shaw, A. D. Beyer, and A. Faraon, Science **357**, 1392 (2017).

[27] See Supplemental Material at http://link.aps.org/supplemental/10.1103/PhysRevLett.126.047404 for the detailed description of the master equation approach, cross-sectional strain distribution of the resonator, peak broadening in the time-integrated measurement, experimental feasibility of the blue-detuned pump, and design of the

resonator in the strong coupling regime, which includes Refs. [28–30].
[28] F. Marquardt, J. P. Chen, A. A. Clerk, and S. M. Girvin, Phys. Rev. Lett. **99**, 093902 (2007).
[29] C. W. Thiel, T. Böttger, and R. L. Cone, J. Lumin. **131**, 353 (2011).
[30] K. Mølmer, Y. Le Coq, and S. Seidelin, Phys. Rev. A **94**, 053804 (2016).
[31] M. W. Doherty, V. V. Struzhkin, D. A. Simpson, L. P. McGuinness, Y. Meng, A. Stacey, T. J. Karle, R. J. Hemley, N. B. Manson, L. C. L. Hollenberg, and S. Prawer, Phys. Rev. Lett. **112**, 047601 (2014).
[32] I. Wilson-Rae, P. Zoller, and A. Imamoglu, Phys. Rev. Lett. **92**, 075507 (2004).
[33] D. Hu, S. Y. Huang, J. Q. Liao, L. Tian, and H. S. Goan, Phys. Rev. A **91**, 013812 (2015).
[34] S. Gröblacher, K. Hammerer, M. R. Vanner, and M. Aspelmeyer, Nature (London) **460**, 724 (2009).
[35] E. Verhagen, S. Deléglise, S. Weis, A. Schliesser, and T. J. Kippenberg, Nature (London) **482**, 63 (2012).
[36] X. Xu, V. Fili, W. Szuba, M. Hiraishi, T. Inaba, T. Tawara, H. Omi, and H. Gotoh, Opt. Express **28**, 14448 (2020).
[37] P. Cao, R. Betzholz, and J. Cai, Phys. Rev. B **98**, 165404 (2018).